Closed formulas for ground band energies of nuclei with various symmetries

2010 J. Phys. G: Nucl. Part. Phys. 37 085108

(http://iopscience.iop.org/0954-3899/37/8/085108)

IOP PUBLISHING JOURNAL OF PHYSICS G: NUCLEAR AND PARTICLE PHYSICS

J. Phys. G: Nucl. Part. Phys. **37** (2010) 085108 (25pp) doi:10.1088/0954-3899/37/8/085108

Closed formulas for ground band energies of nuclei with various symmetries

A A Raduta[1,2], R Budaca[1] and Amand Faessler[3]

[1] Institute of Physics and Nuclear Engineering, Bucharest, POB MG6, Romania
[2] Academy of Romanian Scientists, 54 Splaiul Independentei, Bucharest 050094, Romania
[3] Institüt für Theoretische Physik der Universität Tübingen, Auf der Morgenstelle 14, D-72076 Tübingen, Germany

E-mail: raduta@nipne.ro, apolodor.raduta@uni-tuebingen.de

Received 12 April 2010
Published 28 June 2010
Online at stacks.iop.org/JPhysG/37/085108

Abstract

A time-dependent variational principle is used to dequantize a second-order quadrupole boson Hamiltonian. The classical equations for the generalized coordinate and the constraint for the angular momentum are quantized and then analytically solved. A generalized Holmberg–Lipas formula for energies is obtained. A similar $J(J+1)$ dependence is provided by the coherent state model in the large deformation regime, by using an expansion in powers of $1/x$ for energies, with x denoting a deformation parameter squared. A simple compact expression is also possible for the near-vibrational regime. These three expressions have been used for 44 nuclei covering regions characterized by different dynamic symmetries or in other words belonging to all the known nuclear phases. Nuclei satisfying the specific symmetries of the critical point in the phase transitions $O(6) \rightarrow SU(3)$, $SU(5) \rightarrow SU(3)$ have also been considered. The agreement between the results and the corresponding experimental data is very good. This is reflected in very small root mean square values of deviations.

1. Introduction

One of the big merits of the liquid drop model is that it defines in a consistent way the rotational bands. Many theoretical efforts have been made for the description of excitation energies as well as of electromagnetic transition probabilities. One of the early claims was to obtain a closed formula for the ground state band energies which explains the deviations from the $J(J+1)$ pattern. Various methods have been proposed which were mainly based on the principle of variable moment of inertia [1–3]. These approaches proposed for ground band energies are a series expansion in terms of $J(J+1)$. The weak point of these expansions is that they do not converge for high angular momenta. The first attempt to avoid this difficulty

was made by Holmberg and Lipas [4] who proposed a square root of a linear expression of $J(J+1)$. This expression proves to work better than a quadratic expression in $J(J+1)$.

Here we address the question whether this formula can be improved such that it could be extended to the region of states with high angular momenta. In the present paper we offer three solutions for this problem, each of them being obtained in a distinct manner. One solution is based on a semiclassical treatment of a second-order quadrupole boson Hamiltonian. The remaining two expressions for the ground band energies are given by asymptotic and near-vibrational expansions, respectively, of an angular momentum projection formula. The three expressions obtained for energies are used for a large number of nuclei. The above-sketched project has been achieved according to the following plan. In section 2 we present the semiclassical approach in connection with a quadratic quadrupole boson Hamiltonian. In section 3 the angular momentum projection method is described. Numerical applications are presented in section 4, while the final conclusions are drawn in section 5.

2. Semiclassical treatment of a second-order quadrupole boson Hamiltonian

For a moment we consider the simplest quadrupole boson $\left(b^{\dagger}_{2,\mu}, -2 \leqslant \mu \leqslant 2\right)$ Hamiltonian:

$$H = A_1 \sum_{\mu} b^{\dagger}_{\mu} b_{\mu} + A_2 \sum_{\mu} \left(b^{\dagger}_{\mu} b^{\dagger}_{-\mu} + b_{\mu} b_{-\mu}\right)(-)^{\mu}. \tag{2.1}$$

Here, we are interested in studying the classical equations provided by the time-dependent variational principle associated with H:

$$\delta \int \langle \Psi | H - \mathrm{i}\hbar \frac{\partial}{\partial t} | \Psi \rangle \, \mathrm{d}t = 0. \tag{2.2}$$

If the variational states span the whole Hilbert space of boson states, then solving the variational equations is equivalent to solving the time-dependent Schrödinger equation, which is in general a difficult task. Therefore, we restrict the trial function to a coherent state which we hope is a suitable state for describing the semiclassical feature of the chosen system:

$$|\Psi\rangle = \exp\left[z_0 b^{\dagger}_0 - z^*_0 b_0 + z_2\left(b^{\dagger}_2 + b^{\dagger}_{-2}\right) - z^*_2 (b_2 + b_{-2})\right]|0\rangle. \tag{2.3}$$

Indeed the coherence property results from the obvious equation satisfied by $|\Psi\rangle$:

$$b_{\mu}|\Psi\rangle = (\delta_{\mu 0} z_0 + (\delta_{\mu 2} + \delta_{\mu -2}) z_2)|\Psi\rangle. \tag{2.4}$$

In order to write explicitly the equations emerging from (2.2) we have to calculate first the averages of H:

$$\mathcal{H} = \langle \Psi | H | \Psi \rangle, \tag{2.5}$$

as well as of the action operator $-\mathrm{i}\hbar \frac{\partial}{\partial t}$. The variational equation (2.2) yields the following classical equations for the complex coordinates z_k and z^*_k:

$$\begin{aligned} \frac{\partial \mathcal{H}}{\partial z_0} &= -\mathrm{i}\hbar \dot{z}^*_0, \qquad & \frac{\partial \mathcal{H}}{\partial z^*_0} &= \mathrm{i}\hbar \dot{z}_0, \\ \frac{\partial \mathcal{H}}{\partial z_2} &= -2\,\mathrm{i}\hbar \dot{z}^*_2, \qquad & \frac{\partial \mathcal{H}}{\partial z^*_2} &= 2\,\mathrm{i}\hbar \dot{z}_2. \end{aligned} \tag{2.6}$$

Note that the coordinates z_k and z^*_k define a classical phase space while $\mathcal{H}$ plays the role of a classical Hamilton function. In what follows it is useful to bring these equations to a canonical form. This is achieved by the transformation

$$q_i = 2^{(k+2)/4} \mathrm{Re}(z_k), \qquad p_i = \hbar 2^{(k+2)/4} \mathrm{Im}(z_k), \qquad k = 0, 2, \qquad i = \frac{k+2}{2}. \tag{2.7}$$

Indeed, in the new coordinates the classical equations of motion become

$$\frac{\partial \mathcal{H}}{\partial q_k} = -\dot{p}_k, \qquad \frac{\partial \mathcal{H}}{\partial p_k} = \dot{q}_k. \tag{2.8}$$

In terms of the new coordinates, the Hamilton function is written as

$$\begin{aligned}\mathcal{H} &= \frac{A_1 + 2A_2}{2}\left(q_1^2 + q_2^2\right) + \frac{A_1 - 2A_2}{2\hbar^2}\left(p_1^2 + p_2^2\right) \\ &= \frac{A}{2}\left(q_1^2 + q_2^2\right) + \frac{A'}{2\hbar^2}\left(p_1^2 + p_2^2\right),\end{aligned} \tag{2.9}$$

where $A = A_1 + 2A_2$ and $A' = A_1 - 2A_2$. Equations (2.8) provide the connection between the generalized momenta and the coordinate time derivatives:

$$p_1 = \frac{\hbar^2 \dot{q}_1}{A'}, \qquad p_2 = \frac{\hbar^2 \dot{q}_2}{A'}. \tag{2.10}$$

Taking into account these relations, the classical energy function becomes

$$\mathcal{H} = \frac{\hbar^2}{2A'}\left(\dot{q}_1^2 + \dot{q}_2^2\right) + \frac{A}{2}\left(q_1^2 + q_2^2\right). \tag{2.11}$$

In what follows it is useful to use the polar coordinates

$$q_1 = r\cos\theta, \qquad q_2 = r\sin\theta, \tag{2.12}$$

for the Hamilton function

$$\mathcal{H} = \frac{\hbar^2}{2A'}(\dot{r}^2 + r^2\dot{\theta}^2) + \frac{A}{2}r^2. \tag{2.13}$$

The classical system described by $\mathcal{H}$ is exactly solvable since the number of degrees of freedom is equal to the number of constants of motion. Indeed, taking the time derivatives of $\mathcal{H}$ and $\mathcal{L}_3$, the third component of a pseudo-angular momentum acting in a fictitious boson space, one obtains

$$\dot{\mathcal{H}} = 0, \qquad \dot{\mathcal{L}}_3 = 0. \tag{2.14}$$

The components of the pseudo-angular momentum are defined in appendix A. Here, we need the conserved component

$$\mathcal{L}_3 = \tfrac{1}{2}(q_1 p_2 - q_2 p_1). \tag{2.15}$$

Its constant value is conventionally taken to be

$$\frac{\hbar^2}{2A'}r^2\dot{\theta} = L\hbar, \tag{2.16}$$

which allows us to express the angular variable derivative in terms of the radial one:

$$\dot{\theta} = \frac{2A'L}{\hbar r^2}. \tag{2.17}$$

Thus, the energy function written in the reduced space becomes

$$\mathcal{H} = \frac{\hbar^2}{2A'}\dot{r}^2 + \frac{2A'L^2}{r^2} + \frac{A}{2}r^2 \equiv \frac{\hbar^2}{2A'}\dot{r}^2 + V_{\rm eff}(r). \tag{2.18}$$

We recognize the effective potential energy

$$V_{\rm eff}(r) = \frac{2A'L^2}{r^2} + \frac{A}{2}r^2, \tag{2.19}$$

just as the Davidson potential [5].

Instead of solving the classical trajectories and then quantizing them, here we first quantize the energy by replacing

$$\frac{\hbar^2\dot{r}}{A'} \to -\mathrm{i}\hbar\frac{\partial}{\partial r}. \tag{2.20}$$

Thus, one arrives at the Schrödinger equation

$$\left[-\frac{A'}{2}\frac{\partial^2}{\partial r^2} + \frac{2A'L^2}{r^2} + \frac{A}{2}r^2\right]u(r) = \epsilon u(r). \tag{2.21}$$

Making use of the change of variable and function

$$x = \sqrt{\frac{A}{A'}}r^2, \qquad u(r) = \mathrm{e}^{-\frac{x}{2}}x^s f(x), \tag{2.22}$$

one obtains the following differential equation:

$$\left[x\frac{\partial^2}{\partial x^2} + \left(2s + \frac{1}{2} - x\right)\frac{\partial}{\partial x} + \left(\frac{2s^2 - s - 2L^2}{2x} + \frac{\epsilon}{2\sqrt{AA'}} - \frac{1}{4} - s\right)\right]f(x) = 0. \tag{2.23}$$

This should be compared with the differential equation for the Laguerre polynomials:

$$\left[x\frac{\partial^2}{\partial x^2} + (m + 1 - x)\frac{\partial}{\partial x} + n\right]L_n^m(x) = 0. \tag{2.24}$$

Indeed, the two equations are identical provided the following equations hold:

$$1 + m = 2s + \frac{1}{2}, \qquad n = \frac{\epsilon}{2\sqrt{AA'}} - \frac{1}{4} - s, \qquad 2s^2 - s - 2L^2 = 0. \tag{2.25}$$

From the last equation we derive the expression of s as a function of L. The positive solution is

$$s = \tfrac{1}{4}(1 + \sqrt{1 + 16L^2}). \tag{2.26}$$

The second equation (2.25) yields for the energy ϵ the following expression:

$$\epsilon = 2\sqrt{\left(A_1^2 - 4A_2^2\right)}\left(n + \tfrac{1}{2} + \tfrac{1}{4}\sqrt{1 + 16L^2}\right), \qquad n = 0, 1, 2, \ldots, \qquad L = 0, 1, 2, \ldots. \tag{2.27}$$

An approximate expression may be obtained by expanding first the Davidson potential V_{eff} around its minimum r_0 given by the equation

$$r_0^2 = 2L\sqrt{\frac{A'}{A}}, \tag{2.28}$$

and truncating the expansion at the quadratic term. The result for the energy function is

$$\mathcal{H} = \frac{\hbar^2}{2A'}\dot{r}^2 + 2A(r - r_0)^2 + 2L\sqrt{AA'}. \tag{2.29}$$

Quantizing this Hamilton function we obtain an eigenvalue equation for a harmonic oscillator whose energy is

$$E_{nL} = 2\sqrt{AA'}\left(n + \tfrac{1}{2}\right) + 2L\sqrt{AA'} = 2\sqrt{\left(A_1^2 - 4A_2^2\right)}\left(n + \tfrac{1}{2} + L\right), \qquad n = 0, 1, 2, \ldots. \tag{2.30}$$

We remark the fact that the two spectra coincide when L is large:

$$E_{nL} \approx \epsilon_{n,L}, \qquad \text{for} \quad L = \text{large}. \tag{2.31}$$

Note that the initial boson Hamiltonian could easily be diagonalized by a suitable chosen canonical transformation

$$\tilde{b}^{\dagger}_{\mu} = Ub^{\dagger}_{\mu} - V(-)^{\mu}b_{-\mu}, \qquad \tilde{b}_{\mu} = Ub_{\mu} - V(-)^{\mu}b^{\dagger}_{-\mu}. \tag{2.32}$$

Indeed, the coefficients U and V may be chosen such that

$$\left[\tilde{b}_{\mu}, \tilde{b}^{\dagger}_{\mu'}\right] = \delta_{\mu\mu'}, \qquad \left[H, \tilde{b}^{\dagger}_{\mu}\right] = E\tilde{b}^{\dagger}_{\mu}. \tag{2.33}$$

The second equation provides a homogeneous system of equations for the transformation coefficients

$$\begin{pmatrix} A_1 & 2A_2 \\ -2A_2 & -A_1 \end{pmatrix}\begin{pmatrix} U \\ V \end{pmatrix} = E\begin{pmatrix} U \\ V \end{pmatrix}, \tag{2.34}$$

which determine U and V up to a multiplicative constant which is fixed by the first equation which gives

$$U^2 - V^2 = 1. \tag{2.35}$$

The compatibility condition for equation (2.34) gives $E = \sqrt{A_1^2 - 4A_2^2}$, and therefore the eigenvalues of H are

$$E_n = \sqrt{A_1^2 - 4A_2^2}\left(n + \tfrac{5}{2}\right). \tag{2.36}$$

The frequency obtained is half the one obtained through the semiclassical approach. The reason is that here the frequency is associated with each of the five degrees of freedom while semiclassically the frequency is characterizing a plane oscillator. Note that the pseudo-angular momentum L is different from the angular momentum in the laboratory frame describing rotations in the quadrupole boson space

$$\hat{J}_{\mu} = \sqrt{6}\left(b^{\dagger}_2 b_2\right)_{1\mu}. \tag{2.37}$$

The expected value of the angular momentum square is

$$\langle\Psi|\hat{J}^2|\Psi\rangle = 2\left[q_1^2 + q_2^2 + \frac{1}{\hbar^2}\left(p_1^2 + p_2^2\right)\right]. \tag{2.38}$$

Since the variational function $|\Psi\rangle$ is not the eigenstate of $\hat{J}^2$, the above-mentioned average value is not a constant of motion. Indeed, it is easy to check that

$$\frac{\partial\langle\Psi|\hat{J}^2|\Psi\rangle}{\partial t} = \frac{6}{\hbar^2}(A' - A)(q_1p_1 + q_2p_2) \neq 0. \tag{2.39}$$

It is instructive to see whether we could crank the system so that the magnitude of the angular momentum is preserved, i.e.

$$\langle\Psi|\hat{J}^2|\Psi\rangle = \hbar^2 J(J+1). \tag{2.40}$$

Using polar coordinates the above equation becomes

$$\frac{3\hbar^2}{A'^2}\dot{r}^2 + \frac{12L^2}{r^2} + 3r^2 = J(J+1). \tag{2.41}$$

This equation is treated similarly to the energy equation. Thus, by the quantization

$$\frac{A'^2}{\hbar^2}\dot{r} \to -\mathrm{i}\hbar\frac{\partial}{\partial r}, \tag{2.42}$$

equation (2.41) becomes a differential equation for the wavefunction describing the angular momentum:

$$-\frac{\partial^2\Phi}{\partial r^2} + \left(\frac{4L^2}{A'^2r^2} + \frac{r^2}{A'^2}\right)\Phi = \frac{J(J+1)}{3A'^2}\Phi. \tag{2.43}$$

Making the change of variable and function

$$x = \frac{r^2}{A'}, \qquad \Phi = \mathrm{e}^{-\frac{x}{2}} x^s \Psi, \tag{2.44}$$

we obtain the following equation for Ψ:

$$x\frac{\partial^2\Psi}{\partial x^2} + \left(2s - x + \frac{1}{2}\right)\frac{\partial\Psi}{\partial x} + \left(\frac{2s^2 - s - \frac{2L^2}{A'^2}}{2x} + \frac{J(J+1)}{12A'} - s - \frac{1}{2}\right)\Psi = 0. \tag{2.45}$$

This equation admits the Laguerre polynomials $L_{n'}^{m'}(x)$ with the quantum numbers determined as follows:

$$m' = 2s - \frac{1}{2}, \qquad s = \frac{1}{4} + \frac{1}{4}\sqrt{1 + \frac{16L^2}{A'^2}}, \qquad \frac{J(J+1)}{12A'} = n' + \frac{1}{2} + \frac{1}{4}\sqrt{1 + \frac{16L^2}{A'^2}}. \tag{2.46}$$

The last relation (2.46) can be viewed as an equation determining L:

$$L = \left[\left(\frac{J(J+1)}{12} - A'\left(n' + \frac{1}{2}\right)\right)^2 - \left(\frac{A'}{4}\right)^2\right]^{1/2}. \tag{2.47}$$

On the other hand taking the harmonic approximation for the potential term in equation (2.41) one obtains the classical equation for a harmonic oscillator from which we get

$$J(J+1) = 12A'\left(n' + \tfrac{1}{2}\right) + 12L. \tag{2.48}$$

Reversing this equation one can express the pseudo-angular momentum L in terms of the angular momentum J:

$$L = \frac{J(J+1)}{12} - A'\left(n' + \frac{1}{2}\right). \tag{2.49}$$

Replacing, successively, the expressions for L (2.47), (2.49) into energy equations (2.27), (2.30), we obtain four distinct expressions for the energies characterizing the starting Hamiltonian H:

$$E^{(1)}_{nn'J} = \sqrt{AA'}\left[2n + 1 + \frac{J(J+1)}{6} - A'(2n'+1)\right], \tag{2.50}$$

$$E^{(2)}_{nn'J} = \sqrt{AA'}\left[2n + 1 + 2\sqrt{\left[\frac{J(J+1)}{12} - A'\left(n' + \frac{1}{2}\right)\right]^2 - \left(\frac{A'}{4}\right)^2}\right], \tag{2.51}$$

$$E^{(3)}_{nn'J} = \sqrt{AA'}\left[2n + 1 + \frac{1}{2}\sqrt{1 + 4\left[\frac{J(J+1)}{6} - A'(2n'+1)\right]^2}\right], \tag{2.52}$$

$$E^{(4)}_{nn'J} = \sqrt{AA'}\left[2n + 1 + \frac{1}{2}\sqrt{1 + 4\left[\frac{J(J+1)}{6} - A'(2n'+1)\right]^2 - (A')^2}\right]. \tag{2.53}$$

Note the fact that for a fixed pair of (n, n') each of the above equations defines a rotational band: the lowest band corresponds to $(n, n') = (0, 0)$ and defines the ground band. Except for the band energies $E^{(1)}_{00J}$, which exhibit a $J(J+1)$ pattern, the other three bands have the same generic expressions. Thus, the excitation energies have the form

$$E_J = a[\sqrt{1 + bJ(J+1) + cJ^2(J+1)^2} - 1], \tag{2.54}$$

which is a generalization of the Holmberg–Lipas formula [4]. The results presented with this formula in section 4 are obtained with theory (2). The parameters a, b and c will be fitted by three different energy levels.

We recall that we required that the average value of $\hat{J}^2$ equals $\hbar^2 J(J+1)$. Subsequently, we eliminated the energy dependence on the pseudo-angular momentum L. In this way we projected approximately the angular momentum from the variational state. In the next section we shall show that the exact treatment of the angular momentum projection also yields a closed formula for energy as a function of $J(J+1)$.

3. The method of angular momentum projected state

For the sake of simplicity here we consider a simple form for the variational state

$$|\Psi_g\rangle = \mathrm{e}^{d(b^\dagger_{20}-b_{20})}|0\rangle, \tag{3.1}$$

in connection with the following quadrupole boson Hamiltonian:

$$H = A_1 \sum_\mu b^\dagger_{2\mu} b_{2\mu} + A_2 \hat{J}^2. \tag{3.2}$$

The vacuum state for the quadrupole boson operators is denoted by $|0\rangle$ while d is a real quantity which plays the role of the deformation parameter. The reason is the fact that the average value of the quadrupole moment, written in the lowest order in terms of the quadrupole boson operator, with the function $|\Psi_g\rangle$, is proportional to d. The component of a given angular momentum is obtained by a projection procedure

$$\varphi^{(g)}_{JM} = N^{(g)}_J P^J_{M0} \Psi_g, \tag{3.3}$$

where P^J_{MK} denotes the angular momentum projection operator:

$$P^J_{MK} = \frac{2J+1}{8\pi^2} \int D^{J*}_{MK}(\Omega) \hat{R}(\Omega)\, \mathrm{d}\Omega, \tag{3.4}$$

with D^{J*}_{MK} denoting the Wigner functions and $\hat{R}(\Omega)$ a rotation defined by the Euler angle Ω. The system energy is defined as the average value of H with the projected state

$$E^{(g)}_J \equiv \left\langle \varphi^{(g)}_{JM} \middle| H \middle| \varphi^{(g)}_{JM} \right\rangle = A_1 d^2 \frac{I^{(1)}_J(d^2)}{I^{(0)}_J(d^2)} + A_2 J(J+1), \tag{3.5}$$

where we denoted by $I^{(0)}_J$ the overlap integral:

$$I^{(0)}_J(x) = 2\int_0^1 P_J(y)\, \mathrm{e}^{x P_2(y)}\, \mathrm{d}y, \qquad x = d^2. \tag{3.6}$$

The kth derivative of this integral is denoted by

$$I^{(k)}_J(x) = \frac{\mathrm{d}^k I^{(0)}_J}{\mathrm{d}x^k}. \tag{3.7}$$

The normalization constant for the projected state has the expression

$$\left(N^{(g)}_J\right)^{-2} = (2J+1) I^{(0)}_J\, \mathrm{e}^{-d^2}. \tag{3.8}$$

These integrals have been analytically calculated in [13]. Actually the energies presented here refer to the ground band described by the coherent state model (CSM) which considers simultaneously three interacting bands: ground, beta and gamma. In the asymptotic limit of the deformation parameter d, the ground band energies have the expression [6]

$$E^{(g,\mathrm{asym})}_J = \frac{A_1}{2}\left[\frac{x-1}{2} + G^{1/2}_J\right] + A_2 J(J+1), \tag{3.9}$$

Table 1. The smallest value of d, for which G_J is positive.

J	0	2	4	6	8	10	12	14	16	18	20	22	24	26	28	30
$d_{\min}$	1.55	0	0	0.65	1.21	1.43	1.59	1.71	1.82	1.91	1.99	2.07	2.14	2.21	2.27	2.33

with

$$G_J = \frac{9}{4}x(x-2) + \left(J+\frac{1}{2}\right)^2 - \frac{4}{9x}\left(3+\frac{10}{x}+\frac{37}{x^2}\right) + \frac{2}{3x}\left(1+\frac{10}{3x}+\frac{13}{x^2}\right)J(J+1) - \frac{2}{9x^3}J^2(J+1)^2, \qquad x = d^2. \tag{3.10}$$

The parameter $x = d^2$ describes the deformation of the nuclei and is defined in the ansatz for the variational state (3.1). It is worth mentioning that equation (3.9) is similar to the generalized HL formula, with the difference that here the coefficients of the terms $J(J+1)$ and $J^2(J+1)^2$ have explicit expressions in x. Moreover there appears an additional $J(J+1)$ term outside the square root symbol. The expression (3.9) is obtained by replacing the series expansion in $1/x$, associated with the ratio $x\frac{I_J^{(1)}}{I_J^{(0)}}$:

$$x\frac{I_J^{(1)}}{I_J^{(0)}} = x - 1 - \frac{1}{3x} - \frac{5}{9x^2} - \frac{37}{27x^3} + \left(\frac{1}{6x}+\frac{5}{18x^2}+\frac{13}{18x^3}\right)J(J+1) - \frac{1}{54x^3}J^2(J+1)^2 + \mathcal{O}(x^{-4}), \tag{3.11}$$

by a faster convergent one.

According to [7], for the near-vibrational regime (d close to zero) the ground-state band energies have the expressions

$$E_J^{g,\mathrm{vib}} = A_1\left[\frac{J}{2} + \frac{J}{2(2J+3)}x + \frac{9}{2}\frac{(J+1)(J+2)}{(2J+3)^2(2J+5)}x^2 + \frac{27}{2}\frac{(J+1)(J+2)}{(2J+3)^3(2J+5)(2J+7)}x^3\right] + A_2J(J+1). \tag{3.12}$$

For the sake of completeness we present the derivation of the two expressions for the ground band energies, in the rotational and near-vibrational limits, in appendix B.

4. Numerical results

Since expressions (3.9), (3.11) and (3.12) are based on the series expansion in $1/x$ and x, respectively, it is worth showing how far the truncated expansions are from the exact energies. Aiming at this goal in figures 1 and 2 we plotted the ratio $d^2\frac{I_J^{(1)}}{I_J^{(0)}}$ and the associated truncated series for large and small values of d, respectively, as functions of d for the two angular momenta: $J = 12$ and $J = 16$. In the case of the asymptotic regime we also considered the square root expression. In this case one defines an existence interval of d for which $G_J \geqslant 0$. The lower bounds of these intervals for J running from 0 to 30 are listed in table 1. From figure 1 we see that for $d \geqslant 3$ the expressions used for energies achieve convergence even for high angular momenta. Concerning the energies for the near-vibrational regime one notes that we use a power series of x and therefore one may think that such an expansion is valid for $x \leqslant 1$. However, we note that the coefficients of this expansion depend on J and

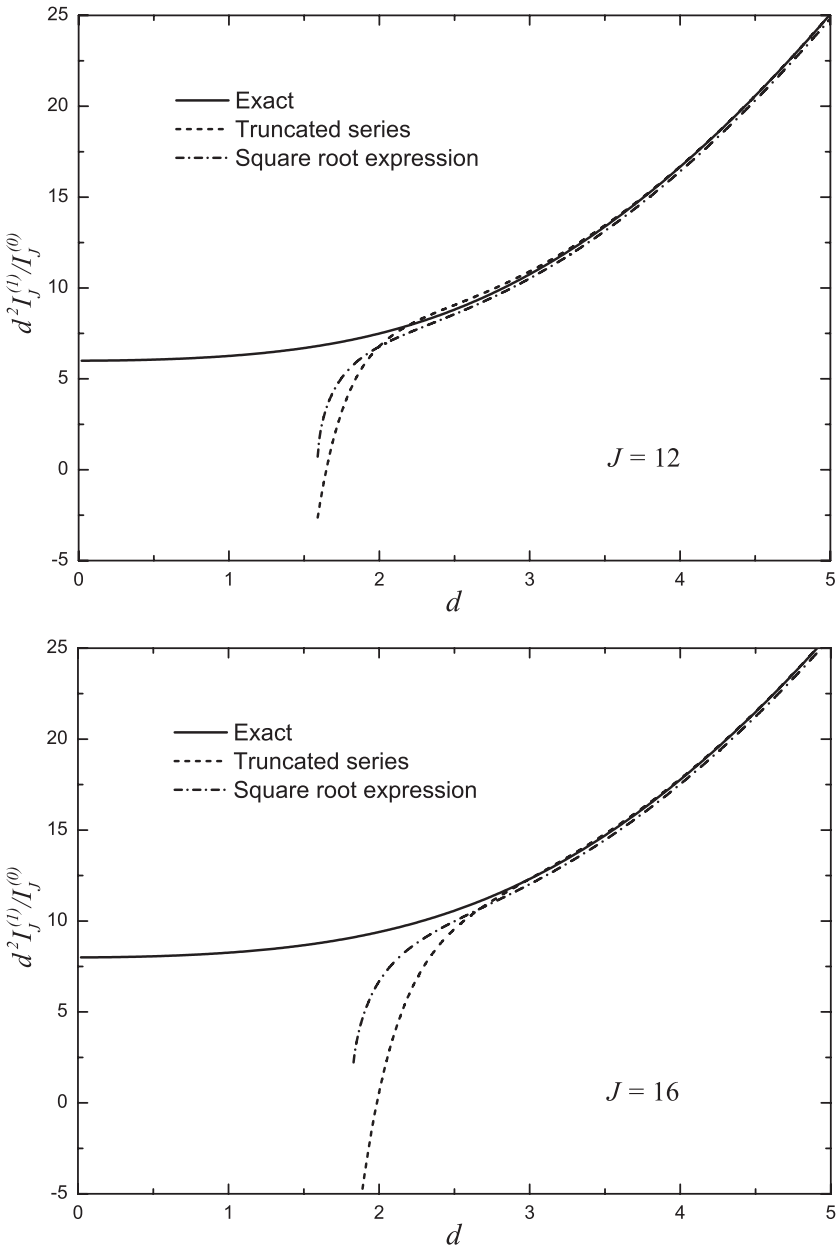

Figure 1. $d^2 I_J^{(1)}/I_J^{(0)}$ is plotted as a function of d for two values of angular momentum. Two approximations of this function are also presented. One is a truncated expansion in $1/x$, while the other one is given by a square root expression which converges slightly faster than the previously mentioned expansion.

moreover are less than unity. The larger the J the smaller are these coefficients. This fact infers that the convergence radius is larger than unity and is an increasing function of the angular momentum. As a matter of fact this is confirmed in the plot shown in figure 2. Comparing the curves from figures 1 and 2 one may say that there is a small interval of d where the

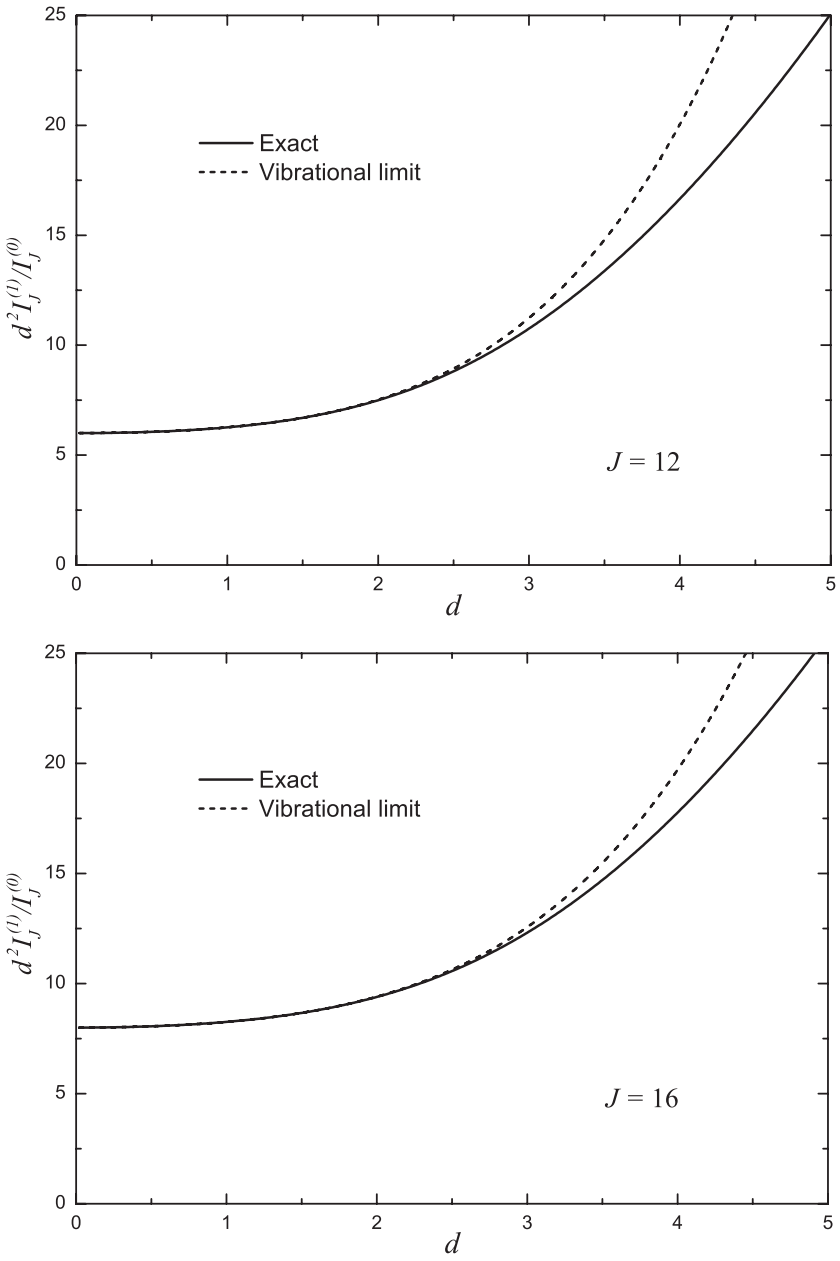

Figure 2. $d^2 I_J^{(1)}/I_J^{(0)}$ is plotted as a function of d for two values of angular momentum. This is compared with the function given by the near-vibrational approximation from equation (3.12).

asymptotic and small x expansions are matched. This allows us to assert that the reunion of the two formulas, (3.9) and (3.12), assures an overall description of nuclei ranging from small to large deformation. In figure 3 we plot the term G_J involved in the energy expression (3.9) as a function of the deformation parameter d. Except for $J = 0$ and $J = 2$ all the other functions vanish for specific values of d which are, in fact, the lower bounds of the existence interval.

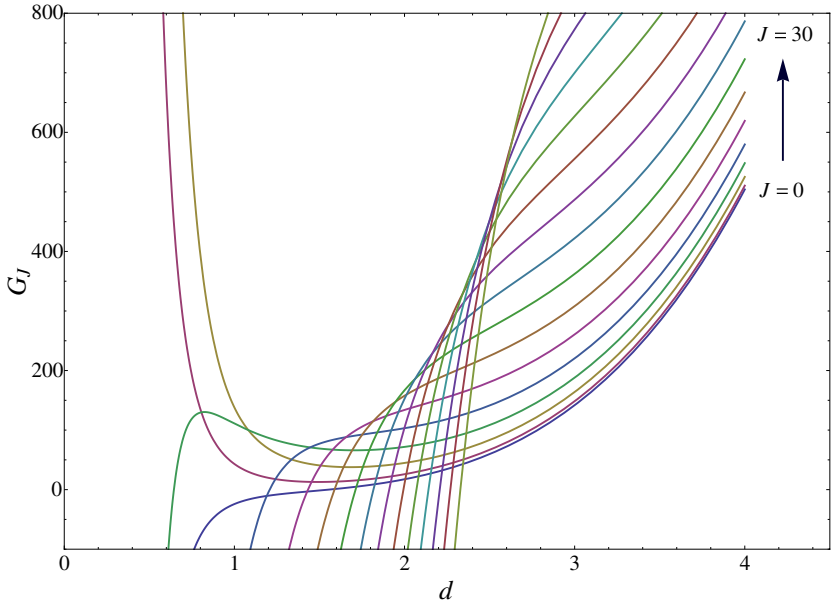

Figure 3. G_J is plotted as a function of d for some angular momenta. Note that except for the cases of $J = 2, 4$, all other functions G_J become negative for d smaller than a critical value. These limiting values are listed in table 1.

(This figure is in colour only in the electronic version)

The basic expressions for energies (2.54), (3.9) and (3.12) have been used for a large number of nuclei grouped according to the nuclear phase to which they belong. Thus, for well-deformed nuclei behaving like axially deformed rotor the ratio E_{4^+}/E_{2^+} should be close to the value of 3.3 while for the near-vibrational region one expects a ratio close to the value 2. Between these two extreme values gamma unstable nuclei are placed, where the ratio may run in the interval 2.5–3.0. The deviation from axial symmetry can affect the ratio mentioned above. Thus, ^{228}Th exhibits some specific feature of a triaxial nucleus with an equilibrium value $\gamma^0 = 30^0$. The corresponding ratio E_{4^+}/E_{2^+} is equal to 3.24. According to the IBA (interacting boson approximation) model [8, 9] the nuclei belonging to the three groups mentioned above are described by the irreducible representations of some dynamic groups such as $SU(3)$, $SU(5)$ and $O(6)$. Since the nuclei described by a certain symmetry group exhibit some specific distinct properties one says that these form a certain nuclear phase. According to Casten [10] all nuclei of the periodic table may be placed on the sides of a triangle having the three symmetries mentioned above at the vertices. On each side which links two adjacent symmetries one expects a critical transition point between the two adjacent phases. A few years ago, Iachello [11, 12] advanced the idea that each of the critical nuclei lying on the three triangle sides correspond to specific symmetries. Thus, the transition $O(6) \rightarrow SU(5)$ is characterized by a critical symmetry which is $E(5)$. Representatives of the $E(5)$ symmetry are ^{104}Ru and ^{102}Pd characterized by the specific ratios $E_{4^+}/E_{2^+} = 2.48, 2.29$, respectively. In the transition $SU(5) \rightarrow SU(3)$, the critical point is close to 3. Such nuclei are ^{150}Nd, ^{152}Sm, ^{154}Gd and ^{156}Dy. Indeed, these prove to be critical points for the mentioned phase transition when the entire isotopic chains are considered.

The question to be answered is whether the compact energy formulas obtained in this paper are able to describe the ground band energies for all nuclei mentioned above. The

theoretical values for energies labeled by Th(1) are obtained with equation (3.9) if d is large or with equation (3.12) when d is smaller than 2. The calculated energies labeled by Th(2) are obtained with equation (2.54). The parameters A_1, A_2, d were obtained by a least mean square fitting procedure while a, b, c by fixing the energies of three particular levels. The fitted energies were chosen such that an overall good agreement with experimental data is obtained. The best set of a, b, c would be obtained by minimizing the rms (root mean square) value of deviations which, for this case, is a more tedious procedure.

The agreement of calculated and experimental excitation energies is judged by the rms values of the deviation, denoted by

$$\chi = \sqrt{\sum_{i}^{N} \frac{(E_i^{\rm Th} - E_i^{\rm Exp})^2}{N}}. \tag{4.1}$$

The fitting procedure yields for the coefficients b and c double precision numbers, which are presented, in tables, in a truncated form. Since the square root formula provides energies which are quite sensitive to small variations for the parameters b and c, we give their values with a suitable large number of digits. Indeed, with the listed parameters we get the energies corresponding to the exact parameters yielded by the fitting procedure. Comparing the values of c for different nuclei, one remarks that the parameter acquires larger values for a smaller deformation parameter. For the two nuclei, ^{248}Cm and ^{180}Os, the parameter c gets negative values which annihilates a part of the contribution coming from the $J(J+1)$ term.

In tables 2 and 3 the results are given for some isotopes of Th, U, Pu and Cm. Except for ^{228}Th, these isotopes are characterized by large values for the deformation parameter d. As we already mentioned, ^{228}Th has features which are specific to the triaxial nuclei. We note the small rms values obtained in these cases.

In tables 4–6 the deformed nuclei belonging to the isotopic chains of Nd, Sm, Gd, Dy, Er, Yb, Hf, W, Os are studied. The first six situations can be viewed as deformed branches of the nuclear phase transition $SU(5) \to SU(3)$ while the last three as the deformed branches of the nuclear phase transition $O(6) \to SU(3)$. The nuclei presented in table 7–9 are characterized by small d and moreover they satisfy the $O(6)$ (table 7), $SU(5)$ (table 8) and $X(5)$ (table 9) symmetries, respectively. For all these nuclei, the defining equation (3.12) has been used. One notes that this formula for the near-vibrational picture describes the excitation energies better than the generalized HL formula. This is reflected by the relative rms values.

In table 10 we present the results for ^{150}Nd, ^{152}Sm and ^{154}Gd. These nuclei play the role of critical points for the phase transitions $SU(5) \to SU(3)$ in the respective isotopic chain [14–17]. The first two are also presented in table 9, where they have been described by a formula obtained for a near-vibrational regime. However, one expects that for nuclei close to the critical point the other formula using an asymptotic expansion in terms of $1/x$ works as well. This is actually confirmed by the data presented in table 10 for the first two nuclei. The isotope ^{154}Gd is supposed to satisfy the so-called $X(5)$ symmetry [14]. Our results show that the ground band energies of this critical nucleus is described quite well by the compact formulas (3.9), (3.12).

In the last table (table 11) we present two nuclei which satisfy the symmetry $E(5)$. These are described with the closed formulas (3.12) and (2.54). We also remark that in this case the rms values are small. For these nuclei, only energies smaller than the value where the first backbending shows up were considered.

Before closing this section we summarize our results presented in tables 2–11. For nuclei characterized by the ratios $E_g^{4^\dagger}/E_g^{2^\dagger}$ larger than 2.93 we have used the asymptotic expansion for energies (equation (3.9)) while for values of this ratio smaller than 3.02 the expansion for

Table 2. Experimental (Exp.) and theoretical (Th(1) and Th(2)) excitation energies for several nuclei, ^{228}Th [18], ^{232}Th [19], ^{232}U [19], ^{234}U [20], ^{236}U [21], ^{238}U [22], are given in units of keV. The predictions labeled by Th(1) are obtained by the square root formula given by the asymptotic expansion of the CSM-ground band energies (equation (3.9)), while Th(2) are obtained by the generalized HL expression (equation (2.54)). The parameters for Th(1) calculations, i.e. A_1, A_2, d, were obtained by a least mean square procedure while those of set Th(2), a, b, c, by fixing three particular energy levels, which are underlined. The obtained parameters are also listed. To have a hint about the agreement between the theoretical and experimental excitation energies, for each case the rms value of discrepancies, denoted by χ, is also given. The values of A_1, A_2, a, χ are given in keV while d, b, c are dimensionless. Having in view a possible classification of the considered nuclei, the ratio $E_g^{4^+}/E_g^{2^+}$ is also given.

		^{228}Th			^{232}Th			^{232}U			^{234}U			^{236}U			^{238}U		
J^π		Exp.	Th(1)	Th(2)	Exp.	Th(1)	Th(2)	Exp.	Th(1)	Th(2)	Exp.	Th(1)	Th(2)	Exp.	Th(1)	Th(2)	Exp.	Th(1)	Th(2)
2^+		57.76	57.61	57.485	49.37	49.66	49.31	47.57	47.46	47.54	43.50	43.72	43.49	45.24	45.516	45.22	44.92	44.73	44.88
4^+		186.82	186.90	186.82	162.12	162.966	162.12	156.57	156.34	156.57	143.35	143.93	143.35	149.48	150.33	149.48	148.38	147.93	148.38
6^+		378.18	378.51	378.78	333.2	334.64	333.63	322.60	322.59	322.96	296.07	296.84	296.07	309.78	311.34	309.97	307.18	306.90	307.71
8^+		622.50	622.73	623.29	556.90	558.25	557.65	541.00	540.94	541.33	497.04	497.63	497.02	522.24	524.29	522.724	518.10	517.8	518.96
10^+		911.80	911.49	911.80	827.0	827.44	827.69	805.80	805.75	805.97	741.2	741.3	741.15	782.3	784.32	783.07	775.9	776.26	777.492
12^+		1239.4	1238.58	1237.99	1137.1	1136.62	1137.77	1111.5	1111.64	1111.5	1023.8	1023.38	1023.69	1085.3	1086.49	1086.07	1076.7	1077.35	1078.41
14^+		1599.5	1599.27	1597.63	1482.8	1481.12	1482.77	1453.7	1453.81	1453.3	1340.8	1339.79	1340.41	1426.3	1426.07	1426.86	1415.5	1416.33	1416.88
16^+		1988.1	1989.81	1988.1	1858.6	1857.14	1858.6	1828.1	1828.13	1827.61	1687.8	1687.24	1687.8	1800.9	1798.79	1800.9	1788.4	1788.68	1788.4
18^+		2407.9	2407.05	2407.9	2262.9	2261.56	2262.1	(2231.5)	2231.13	2231.5	2063.0	2062.99	2063.08	2203.9	2200.85	2204.11	2191.1	2190.24	2188.89
20^+			2848.18	2856.32	2691.5	2691.82	2690.9	(2659.7)	2659.9	2662.76	2464.2	2464.74	2464.12	2631.7	2628.97	2632.91	2619.1	2617.29	2614.76
22^+			3310.53	3333.13	3144.2	3145.71	3143.29		3111.96	3119.8	2889.7	2890.57	2889.32	3081.2	3080.31	3084.22	3068.1	3066.53	3062.93
24^+			3791.4	3838.43	3619.6	3621.32	3618.06		3585.21	3601.5	3339	3338.8	3337.54	(3550)	3552.43	3555.4	3535.3	3535.05	3530.78
26^+			4287.89	4372.51	4116.2	4116.88	4114.4		4077.8	4107.12	3808	3807.96	3808.0	(4039)	4043.2	4044.28	4018.1	4020.31	4016.08
28^+			4796.81	4935.76	(4631.8)	4630.77	4631.8		4588.11	4636.2	(4297)	4296.74	4300.17	(4549)	4550.77	4549.0	4517	4520.08	4517.0
30^+			5314.41	5528.64	(5162)	5161.41	5169.96		5114.65	5188.48		4803.88	4813.74	(5077)	5073.52	5068.04	5035	5032.4	5031.98
$\frac{E_g^{4^+}}{E_g^{2^+}}$		3.23			3.28			3.29			3.30			3.30			3.30		
χ			0.56	0.66		1.13	2.2		0.17	1.00		0.53	0.95		2.21	3.16		1.40	2.48
A_1	a	182.8720	1909.4426		233.4401	3339.3037		298.6610	3472.2796		221.7839	3443.7877		386.4548	5932.3853		502.4456	5945.5847	
A_2	b	4.0861	0.010 1534		3.2430	0.004 952 22		2.6094	0.004 588 75		2.9879	0.004 230 38		1.9129	0.002 549 85		1.0667	0.002 525 36	
d	c	2.7062	$5.470\,7523 \times 10^{-6}$		3.0822	$1.026\,518 \times 10^{-6}$		3.3385	$1.102\,772 \times 10^{-6}$		3.2192	$9.425\,528 \times 10^{-7}$		3.6189	$7.754\,542 \times 10^{-8}$		3.8524	$6.979\,548 \times 10^{-8}$	

Table 3. The same as table 2 but for a different set of nuclei: ^{236}Pu [21], ^{238}Pu [22], ^{240}Pu [23], ^{242}Pu [24], ^{248}Cm [25].

		^{236}Pu			^{238}Pu			^{240}Pu			^{242}Pu			^{248}Cm		
J^π		Exp.	Th(1)	Th(2)	Exp.	Th(1)	Th(2)	Exp.	Th(1)	Th(2)	Exp.	Th(1)	Th(2)	Exp.	Th(1)	Th(2)
2^+		44.63	44.514	44.602	44.076	43.818	44.06	42.824	42.88	42.82	44.54	44.14	44.49	43.40	43.41	43.33
4^+		147.45	147.23	147.45	145.95	145.25	145.95	141.69	141.84	141.69	147.3	146.29	147.3	143.6	143.80	145.6
6^+		305.80	305.55	305.82	303.38	302.44	303.61	294.32	294.52	249.34	306.4	304.52	306.20	298.1	299.18	298.88
8^+		515.7	515.80	515.939	513.58	512.76	514.16	497.52	497.73	497.61	518.1	516.00	517.98	505.0	506.59	506.30
10^+		773.5	773.6	773.5	773.48	773.027	774.231	(747.8)	747.93	747.93	778.6	777.19	778.86	760.7	762.36	762.29
12^+		1074.3	1074.31	1074.1	1080.1	1079.84	1080.33	(1041.8)	1041.61	1041.71	1084.4	1084.14	1084.78	1061.3	1062.39	1062.77
14^+		1413.6	1413.31	1413.6	1429.1	1429.73	1429.1	(1375.6)	1375.54	1375.6	1431.7	1432.67	1431.7	1402.5	1402.35	1403.35
16^+		1786.0	1786.21	1788.29	1818.5	1819.41	1817.49	(1746.9)	1746.84	1746.67	1816.7	1818.59	1815.83	1779.6	1777.89	1779.6
18^+			2188.99	2195.01	2244.9	2245.79	2242.86	(2153.1)	2153.04	2152.48	2236.0	2237.82	2233.73	2187.7	2184.82	2187.09
20^+			2618.05	2631.13	2705.7	2706.08	2703.0	(2591.9)	2592.01	2591.07	2686	2686.51	2682.38	2621.5	2619.16	2621.59
22^+			3070.18	3094.55	3198.8	3197.78	3196.12	(3062.2)	3061.95	3060.93	3163	3161.07	3159.2	3077.2	3077.22	3079.06
24^+			3552.59	3583.61	3720.8	3718.68	3720.8	(3560.9)	3561.32	3560.9	3662	3658.24	3662.0	3552.4	3555.65	3555.75
26^+			4032.81	4097.01	4265.2	4266.82	4275.97	(4089)	4088.78	4090.18	4172	4175.02	4188.99	4048.2	4051.4	4048.2
28^+			4538.68	4633.81		4840.48	4860.82		4643.16	4648.2		4708.76	4738.69	4564.5	4561.71	4553.19
30^+			5058.3	5193.28		5438.15	5474.79		5223.42	5234.61		5257.04	5309.9		5084.14	5067.79
$\frac{E_g^{4^+}}{E_g^{2^+}}$		3.30			3.31			3.31			3.31			3.31		
χ			0.18	1.72		0.99	3.24		0.19	0.57		1.89	4.98		1.95	3.28
A_1	a	486.0023	4857.3300		397.4155	5443.1075		232.3635	4487.9012		692.5499	6375.5552		705.2236	10 281.7179	
A_2	b	1.2356	0.003 071 87		2.4878	0.002 705 63		3.425 35	0.003 1902		0.3216	0.002 332 68		0.0133	0.001 408 28	
d	c	3.8514	$4.909\,159 \times 10^{-7}$		3.9353	$5.862\,828 \times 10^{-7}$		3.4867	$8.397\,898 \times 10^{-7}$		4.2578	$2.196\,286 \times 10^{-7}$		4.2426	$-9.361\,609 \times 10^{-8}$	

Table 4. The same as table 2 but for a different set of nuclei: ^{154}Nd [26], ^{156}Nd [27], ^{156}Sm [27], ^{158}Sm [28], ^{160}Gd [29], ^{162}Gd [30]. The last energy level of ^{154}Nd is uncertain and thereby it was not involved in the fitting procedure.

		^{154}Nd			^{156}Nd			^{156}Sm			^{158}Sm			^{160}Gd			^{162}Gd		
J^π		Exp.	Th(1)	Th(2)	Exp.	Th(1)	Th(2)	Exp.	Th(1)	Th(2)	Exp.	Th(1)	Th(2)	Exp.	Th(1)	Th(2)	Exp.	Th(1)	Th(2)
2^+		70.8	70.55	70.70	66.9	67.13	67.06	75.89	75.60	75.633	(72.8)	72.75	72.581	75.26	75.153	75.22	72.1	71.73	71.89
4^+		233.2	233.80	233.2	221.8	221.93	221.8	249.71	249.64	249.71	(240.3)	240.538	240.3	248.52	248.34	248.52	237.3	236.94	237.3
6^+		481.9	481.65	282.13	460.4	460.48	460.42	517.07	517.13	517.21	(498.4)	499.16	499.41	514.75	514.77	514.02	490.8	490.93	491.25
8^+		810.1	810.26	810.48	777.9	777.76	777.9	871.9	871.90	871.9	(844.5)	843.26	844.5	867.9	868.0	868.15	827.3	827.32	827.3
10^+		1210.8	1211.23	1210.8	1168.9	1168.57	1168.87	1307.4	1307.72	1307.67	(1266.7)	1267.24	1269.02	1300.7	1300.84	1300.7	1238.9	1239.09	1238.75
12^+		1677.3	1677.3	1676.12	1628.4	1628.05	1628.23	1819.3	1818.97	1819.3	(1765.8)	1765.92	1765.8	1806.3	1806.12	1805.6	1719.5	1719.26	1719.5
14^+		2202.4	2201.89	2200.46	2151.6	2151.99	2151.6	2400.8	2400.87	2402.81	(2334.9)	2334.77	2327.52	2377.3	2377.21	2376.51	2261.3	2261.39	2264.46
16^+		2779.0	2779.24	2779.0	2737.0	2736.83	2735.47		3049.5	3055.43		2969.98	2947.08	3008.1	3008.19	3008.1		2859.77	2869.72
18^+		(3399.3)?	3404.46	3408.08		3379.62	3377.18		3761.62	3775.4		3668.38	3617.8		3693.96	3696.07		3509.48	3532.43
20^+			4073.36	4085.0		4077.89	4074.82		4534.54	4561.74		4427.32	4333.63		4430.11	4437.09		4206.31	4250.64
$\frac{E_g^{4^+}}{E_g^{2^+}}$		3.29			3.32			3.29			3.30			3.30			3.29		
χ			0.32	0.82		0.23	0.57		0.21	0.78		0.60	2.95		0.12	0.40		0.23	1.21
A_1	a	441.8371	5240.0423		241.6860	5338.3543		251.2029	4267.15		259.4635	12 111.9787		485.7106	6680.1981		460.9196	4947.3299	
A_2	b	4.3446	0.004 518 88		6.5982	0.004 202 09		7.4572	0.005 933 71		7.2031	0.002 003 42		4.8487	0.003 768 25		4.5633	0.004 864 69	
d	c	3.4184	$1.524\,693 \times 10^{-6}$		3.245 87	$1.952\,257 \times 10^{-6}$		3.1471	$4.471\,374 \times 10^{-6}$		3.2474	$1.233\,053 \times 10^{-8}$		3.5061	$1.059\,795 \times 10^{-6}$		3.4845	$2.343\,414 \times 10^{-6}$	

Table 5. The same as table 2 but for a different set of nuclei: ^{162}Dy [30], ^{164}Dy [31], ^{166}Er [32], ^{172}Yb [33], ^{174}Yb [34], ^{176}Hf [35].

		^{162}Dy			^{164}Dy			^{166}Er			^{172}Yb			^{174}Yb			^{176}Hf		
J^π		Exp.	Th(1)	Th(2)	Exp.	Th(1)	Th(2)	Exp.	Th(1)	Th(2)	Exp.	Th(1)	Th(2)	Exp.	Th(1)	Th(2)	Exp.	Th(1)	Th(2)
2^+		80.66	80.43	80.59	73.39	73.36	73.37	80.58	81.00	80.54	78.74	78.68	78.71	76.47	76.48	76.48	88.35	88.08	88.23
4^+		265.66	265.25	265.66	242.23	242.21	242.23	264.99	266.16	264.99	260.27	260.18	260.27	253.12	253.13	253.12	290.18	289.78	290.18
6^+		548.52	548.23	548.79	501.32	501.34	501.41	545.45	547.04	545.56	539.98	540.01	540.14	526.03	525.93	525.83	596.82	596.78	597.32
8^+		920.50	921.14	921.53	843.68	843.68	843.79	911.21	912.25	911.35	912.12	912.15	912.27	889.93	889.26	888.97	997.74	997.97	998.37
10^+		1374.80	1374.98	1374.8	1261.3	1261.19	1261.3	1349.64	1349.13	1349.64	1370.07	1370.11	1370.07	1336.00	1336.63	1336.0	(1481.07)	1481.13	1481.07
12^+		1901.3	1901.0	1900.04	1745.9	1745.74	1745.76	1846.6	1845.07	1847.06	(1907.48)	1907.52	1907.22	(1861)	1861.27	1860.23	(2034.67)	2034.29	2033.65
14^+		2492	2491.26	2489.81	2289.6	2289.65	2289.52	2389.4	2388.37	2390.46	(2518.7)	2518.62	2518.17	(2457)	2456.66	2455.3	(2646.6)	2646.49	2645.6
16^+		3138	3138.83	3138.0	(2886.0)	2885.99	2885.77	(2967.4)	2968.66	2967.4	(3198.4)	3198.41	3198.4	(3117)	3116.76	3115.52	(3308.0)	3308.11	3308.0
18^+		3838	3837.79	3839.85	(3528.7)	3528.66	3528.7		3576.94	3566.42		3942.58	3944.38	(3836)	3836.14	3836.0	(4010.8)	4010.9	4013.56
20^+			4583.15	4591.79	(4212.3)	4212.4	4213.49		4205.52	4177.02		4747.52	4753.51	(4610)	4610.05	4612.7		4747.85	4756.41
22^+			5370.65	5391.23		4932.68	4936.22		4847.84	4789.64		5610.15	5623.98		5434.34	5442.38		5513.01	5531.95
24^+			6196.67	6236.35		5685.62	5693.78		5498.26	5355.47		6527.85	6554.61		6305.41	6322.51		6301.26	6336.55
$\frac{E_g^{4^+}}{E_g^{2^+}}$		3.29			3.30			3.29			3.31			3.31			3.28		
χ			0.48	1.10		0.07	0.39		1.14	0.41		0.05	0.22		0.33	1.18		0.23	1.07
A_1	a	530.0578	6153.5266		607.1406	7551.6774		850.8099	9490.2037		383.6380	6605.210 25		587.6927	8756.3360		753.6198	6943.5586	
A_2	b	4.4759	0.004 3870		3.1089	0.003 252 137		0.0142	0.002 844 946		6.6422	0.003 985 87		4.5844	0.002 920 61		2.2576	0.004 260 81	
d	c	3.4126	$1.171\,720 \times 10^{-6}$		3.5835	$3.476\,3788 \times 10^{-7}$		3.501 835	$-6.852\,260 \times 10^{-7}$		3.4108	$1.605\,260 \times 10^{-6}$		3.7067	$5.919\,085 \times 10^{-7}$		3.4441	$2.818\,646 \times 10^{-7}$	

Table 6. The same as table 2 but for a different set of nuclei: ^{182}W [36], ^{186}W [37], ^{178}Os [38], ^{180}Os [39], ^{186}Os [37]. The last energy level of ^{182}W is uncertain and therefore it was not considered in the fitting procedure.

		^{182}W			^{186}W			^{178}Os			^{180}Os			^{186}Os		
J^π		Exp.	Th(1)	Th(2)	Exp.	Th(1)	Th(2)	Exp.	Th(1)	Th(2)	Exp.	Th(1)	Th(2)	Exp.	Th(1)	Th(2)
2^+		100.11	99.55	99.82	122.63	119.61	121.30	131.6	125.48	129.07	132.11	130.643	129.82	137.16	133.67	134.65
4^+		329.43	328.81	329.43	396.55	393.36	396.55	397.7	388.23	397.7	408.62	409.45	408.62	434.09	432.25	434.09
6^+		680.50	680.92	681.50	809.25	809.50	811.02	761.00	751.75	762.39	795.08	795.92	796.33	868.94	870.76	871.64
8^+		1144.4	1146.29	1146.07	1349.20	1352.17	1349.20	1193.80	1188.34	1194.95	1257.44	1256.25	1257.44	1420.94	1422.74	1420.94
10^+		1711.90	1713.7	1711.9	2002.4	2003.71	1998.63	1681.6	1685.41	1681.6	1767.57	1766.71	1766.95	2067.95	2065.64	2061.88
12^+		2372.3	2371.37	2367.76	(2750.9)	2746.52	2750.9	2219.4	2230.28	2216.81	2308.71	2310.46	2308.71	2781.26	2781.84	2781.26
14^+		(3112.3)	3107.73	3103.24	(3562.4)	3564.28	3601.12	2804.3	2812.15	2799.12	2875.0	2874.35	2872.48	3557.7	3557.76	3571.28
16^+		(3909.2)	3912.02	3909.2		4442.48	4546.91	(3429)	3419.0	3429.0		3446.79	3451.67		4382.72	4427.8
18^+		(4747.1)?	4774.46	4777.95		5368.52	5587.55		4035.32	4107.78		4016.34	4041.91		5247.84	5349.05
20^+			5686.41	5703.17		6331.66	6723.24		4637.75	4837.1		4570.48	4640.25		6145.34	6334.65
22^+			6640.27	6679.82		7322.68	7954.72		5183.34	5618.61		5094.27	5244.62		7067.97	7385.08
24^+			7629.42	7703.93		8333.72	9282.96		5554.72	6453.89		5568.28	5853.54		8008.58	8501.28
$\frac{E_g^{4^+}}{E_g^{2^+}}$		3.29			3.23			3.02			3.09			3.16		
χ			2.16	10.84		2.74	14.73		8.34	2.33		1.15	1.39		1.99	5.79
A_1	a	1106.3961	9719.4346		1193.1479	3759.9451		217.4255	1297.2467		398.5784	2299.2478		539.1025	3350.11	
A_2	b	1.7794	0.003 438 44		1.0740	0.010 8515		8.5931	0.034 5814		5.1661	0.019 353 26		6.7316	0.013 6108	
d	c	3.7663	$4.179\,487 \times 10^{-7}$		3.5059	$1.256\,224 \times 10^{-5}$		2.1840	$3.875\,729 \times 10^{-5}$		2.4119	$-1.080\,998 \times 10^{-7}$		2.7518	9.3005×10^{-6}	

Table 7. The same as table 2 but for a different set of nuclei: ^{170}W [40], ^{174}Os [34], ^{178}Os [38], ^{176}Pt [35], ^{178}Pt [38], ^{180}Pt [39]. Also the predictions Th(1) are obtained with expression (3.12) corresponding to the expansion characterized by small d.

		^{170}W			^{174}Os			^{178}Os			^{176}Pt			^{178}Pt			^{180}Pt		
J^π		Exp.	Th(1)	Th(2)	Exp.	Th(1)	Th(2)	Exp.	Th(1)	Th(2)	Exp.	Th(1)	Th(2)	Exp.	Th(1)	Th(2)	Exp.	Th(1)	Th(2)
2^+		156.72	147.91	151.42	158.60	152.02	149.25	131.6	119.27	129.07	264.0	233.81	220.91	(170.1)	149.29	149.75	153.21	143.63	138.40
4^+		462.33	472.55	462.33	435.00	432.32	435.0	397.7	404.65	397.7	564.1	549.32	564.1	(427.1)	426.55	427.1	410.74	414.33	410.74
6^+		875.53	881.93	877.80	777.63	778.99	796.32	761.00	769.78	762.39	905.6	918.39	952.62	(764.6)	779.04	778.67	757.07	765.22	768.11
8^+		1363.40	1356.16	1363.4	1171.93	1177.95	1206.54	1193.8	1196.31	1194.95	1305.7	1332.77	1372.98	(1177.6)	1194.67	1189.99	1181.50	1185.52	1190.82
10^+		1901.5	1888.66	1902.46	1617.5	1624.47	1656.71	1681.6	1678.19	1681.6	1764.8	1789.52	1824.74	(1660.4)	1669.39	1660.4	1674.28	1671.64	1674.28
12^+		2464.3	2476.63	2488.05	2113.8	2116.53	2144.95	2219.4	2212.86	2216.81	2277.0	2287.36	2310.5	(2207.6)	2201.46	2192.86	2229.2	2222.0	2219.37
14^+		(3118.0)	3118.64	3118.0	2656.3	2653.1	2672.04	2804.3	2799.02	2799.12	2833.5	2825.61	2833.5	(2811.9)	2789.99	2790.85	2841.5	2835.83	2828.63
16^+		(3815.9)	3813.9	3792.44	3239.8	3233.59	3239.8	(3429)	3435.95	3429.0	3423.8	3403.88	3396.93	(3457.5)	3434.47	3457.5	3504.8	3512.67	3504.8
18^+			4561.93	4512.55	3861.8	3857.66	3850.29		4123.2	4107.78	4041.80	4021.95	4003.64	(4107.9)	4134.61	4195.33	4252.8	4252.27	4250.34
20^+			5362.43	5279.94	4524.9	4525.07	4505.56		4860.49	4837.1	4690.40	4679.66	4656.13		4890.21	5006.32		5054.43	5067.32
22^+			6215.19	6096.38	5233.0	5235.69	5207.47		5647.65	5618.61	5377.0	5376.91	5356.52		5701.14	5892.01		5919.06	5957.41
24^+			7120.05	6963.58	5987.10	5989.4	5957.69		6484.53	6453.89	6106.60	6113.64	6106.6		6567.32	6853.56		6846.07	6921.93
26^+			8076.93	7883.16	6786.1	6786.12	6757.65		7371.04	7344.39	6878.6	6889.78	6907.87		7488.66	7891.85		7835.39	7961.93
28^+					7628.4	7625.81	7608.61												
30^+					8511.6	8508.41	8511.60												
32^+					9429.7	9433.9	9467.53												
$\frac{E_g^{4^+}}{E_g^{2^+}}$		2.95			2.74			3.02			2.14			2.51			2.68		
χ			8.64	11.98		4.01	23.78		7.20	2.33		17.29	37.15		17.56	31.75		6.15	8.80
A_1	a	301.1197	1404.2605		253.6741	801.1928		260.4042	1297.25		277.2380	407.296		222.5347	551.9787		198.9086	761.038	
A_2	b	6.4525	0.037 682 05		5.3413	0.067 3811		6.1596	0.0346		4.9031	0.227 8488		6.8660	0.100 724 68		7.7625	0.065 0988	
d	c	1.6390	$3.305\,334 \times 10^{-5}$		1.5935	$8.260\,490 \times 10^{-5}$		1.6566	3.88×10^{-5}		1.4494	$3.279\,647 \times 10^{-4}$		1.5878	$3.293\,427 \times 10^{-4}$		1.5869	$1.718\,25 \times 10^{-4}$	

Table 8. The same as table 7 but for a different set of nuclei: ^{108}Te [41], ^{150}Sm [42], ^{152}Gd [43], ^{154}Dy [26].

		^{108}Te			^{150}Sm			^{152}Gd			^{154}Dy		
J^π		Exp.	Th(1)	Th(2)	Exp.	Th(1)	Th(2)	Exp.	Th(1)	Th(2)	Exp.	Th(1)	Th(2)
2^+		625.20	605.01	559.90	333.86	305.14	300.10	344.28	336.40	312.00	334.58	337.10	299.71
4^+		1289.00	1296.67	1289.0	773.24	774.07	773.238	755.40	759.65	755.40	747.04	756.47	747.04
6^+		2047.9	2075.43	2083.78	1278.75	1300.12	1301.78	1227.38	1233.74	1239.98	1224.08	1227.93	1241.06
8^+		2945.0	2936.12	2945.0	1836.87	1857.81	1857.43	1746.78	1747.55	1754.67	1747.82	1741.62	1764.45
10^+		3886.2	3876.53	3883.14	2433.00	2438.50	2433.0	2300.4	2297.09	2300.4	2304.3	2293.98	2315.38
12^+		4909.10	4895.60	4909.10	3048.20	3038.44	3027.07	2883.80	2880.59	2880.62	2892.60	2883.42	2895.80
14^+		5980.3	5992.78	6032.53	(3675.70)	3655.73	3640.20	3499.20	3497.12	3499.20	3508.60	3509.09	3508.60
16^+			7167.72	7261.50	4305.90	4289.29	4273.71	4142.70	4146.16	4159.89	4172.70	4170.53	4156.89
18^+			8420.22	8602.58	4929.20	4938.46	4929.20		4827.39	4866.08	4868.60	4867.44	4843.65
20^+			9750.14	10 061.10	(5592.8)	5602.83	5608.38		5540.59	5620.76	5589.90	5599.64	5571.61
22^+			11 157.40	11 641.10		6282.11	6312.92		6285.64	6426.51	6349.9	6367.01	6343.24
24^+			12 641.90	13 346.10		6976.11	7044.47		7062.43	7285.57	7160.70	7169.45	7160.70
26^+			14 203.70	15 178.60		7684.69	7804.56		7870.89	8199.80	8027.50	8006.90	8025.91
$\frac{E_g^{4^+}}{E_g^{2^+}}$		2.06			2.32			2.19			2.23		
χ			15.74	34.41		16.45	22.54		4.45	14.00		9.74	15.61
A_1	a	580.6812	460.8427		532.8764	635.7440		409.7560	398.91		395.7184	481.5077	
A_2	b	9.6296	0.642 4835		1.7549	0.194 008		3.9253	0.360 103		4.3456	0.270 578	
d	c	1.2510	$1.419\,787 \times 10^{-3}$		1.5563	$7.927\,202 \times 10^{-5}$		1.4306	$4.278\,524 \times 10^{-4}$		1.4135	$2.459\,865 \times 10^{-4}$	

Table 9. The same as table 7 but for a different set of nuclei: ^{150}Nd [42], ^{152}Sm [43], ^{156}Dy [27].

		^{150}Nd			^{152}Sm			^{156}Dy		
J^π		Exp.	Th(1)	Th(2)	Exp.	Th(1)	Th(2)	Exp.	Th(1)	Th(2)
2^+		130.21	122.59	126.16	121.78	107.02	118.00	137.77	83.82	128.88
4^+		381.45	386.14	381.45	366.48	372.03	366.48	404.19	398.35	404.19
6^+		720.4	726.86	722.89	706.88	719.04	709.74	770.44	797.667	786.22
8^+		1129.7	1130.85	1129.70	1125.35	1131.97	1125.35	1215.61	1252.12	1242.82
10^+		1599.00	1593.52	1595.26	1609.23	1605.59	1603.21	1725.02	1752.12	1753.75
12^+		(2119.00)	2112.90	2119.0	2148.51	2137.63	2140.1	2285.88	2293.59	2307.61
14^+		(2682.50)	2687.99	2702.57	(2736.01)	2726.97	2736.01	2887.82	2874.50	2898.42
16^+			3318.23	3348.22	(3362.0)	3372.98	3392.27	3523.3	3493.72	3523.30
18^+			4003.30	4058.16		4075.29	4110.63	4178.10	4150.56	4181.18
20^+			4742.97	4834.33		4833.64	4892.87	4859.00	4844.58	4871.98
22^+			5537.10	5678.39		5647.87	5740.62	5573.00	5575.48	5596.23
24^+			6385.58	6591.67		6517.87	6655.29	6328.70	6343.07	6354.73
26^+			7288.35	7575.26		7443.56	7638.09	7130.30	7147.20	7148.47
28^+			8245.35	8630.02		8424.87	8690.01	7978.50	7987.76	7978.50
30^+			9256.53	9756.66		9461.76	9811.89	8875.90	8864.66	8845.86
$\frac{E_g^{4^+}}{E_g^{2^+}}$		2.93			3.01			2.93		
χ			5.61	7.92		9.84	11.43		23.86	18.45
A_1	a	215.8125	2867.41		221.5088	1187.15		348.6711	1913.4867	
A_2	b	6.7513	0.0513		6.9223	0.0344		4.4983	0.023 1439	
d	c	1.6321	1.17×10^{-4}		1.6640	6.11×10^{-5}		1.7089	$1.051\,357 \times 10^{-5}$	

Table 10. The same as table 2 but for a different set of nuclei: ^{150}Nd [42], ^{152}Sm [43], ^{154}Gd [26].

		^{150}Nd			^{152}Sm			^{154}Gd		
J^π		Exp.	Th(1)	Th(2)	Exp.	Th(1)	Th(2)	Exp.	Th(1)	Th(2)
2^+		130.21	123.45	126.16	121.78	119.14	118.00	123.07	108.23	117.32
4^+		381.45	374.67	381.45	366.48	364.57	366.48	370.99	346.04	370.99
6^+		720.40	717.10	722.89	706.88	704.82	709.74	717.65	689.42	728.47
8^+		1129.70	1130.89	1129.70	1125.35	1123.09	1125.35	1144.43	1117.23	1162.21
10^+		1599.00	1603.40	1595.26	1609.23	1608.64	1603.21	1637.04	1614.03	1654.28
12^+		(2119.00)	2123.44	2119.00	2148.51	2151.71	2140.10	2184.67	2168.74	2194.41
14^+		(2682.5)	2677.98	2702.57	(2736.01)	2740.64	2736.01	2777.30	2772.90	2777.30
16^+			3248.12	3348.22	(3362.0)	3357.92	3392.27	3404.44	3419.34	3400.53
18^+			3798.63	4058.16		3968.95	4110.63	4087.10	4101.33	4063.38
20^+			4221.54	4834.33		4444.16	4892.87	4782.30	4811.93	4766.07
22^+				5678.39			5740.62	5519.50	5543.34	5509.31
24^+				6591.67			6655.29	6294.10	6286.21	6294.10
26^+				7575.26			7638.09	7055.50	7028.36	7121.53
$\frac{E_g^{4^+}}{E_g^{2^+}}$		2.93			3.01			3.01		
χ			4.83	7.92		2.93	11.43		21.22	21.77
A_1	a	151.3419	867.4073		126.4776	1187.1506		274.9237	1950.92	
A_2	b	9.5423	0.051 3027		10.3917	0.034 413 709		7.4351	0.020 573 56	
d	c	2.0284	$1.171\,278 \times 10^{-4}$		2.0136	$6.109\,010 \times 10^{-5}$		2.4767	$1.254\,659 \times 10^{-5}$	

small d, i.e. given by equation (3.12), was used. Within the overlapping interval of d, both formulas are valid.

Table 11. The same as in table 7 but for a different set of nuclei:^{104}Ru [44], ^{102}Pd [45]. These nuclei obey the $E(5)$ symmetry.

		^{104}Ru			^{102}Pd		
J^π		Exp.	Th(1)	Th(2)	Exp.	Th(1)	Th(2)
2^+		358.03	348.13	358.03	556.43	563.02	520.03
4^+		888.49	901.59	910.87	1275.87	1280.12	1275.87
6^+		1556.30	1561.29	1556.30	2111.35	2100.12	2114.71
8^+		2320.30	2303.22	2287.30	3013.06	3006.50	3019.06
10^+		3111.80	3119.23	3111.80	3992.71	3993.31	3992.71
12^+			4005.75	4039.35	5055.10	5057.87	5043.55
14^+			4960.97	5078.09	6179.80	6198.80	6179.80
16^+			5983.88	6234.53	7428.80	7415.32	7408.97
18^+			7073.86	7513.64		8706.93	8737.58
20^+			8230.5	8919.18		10073.30	10171.10
$\frac{E_g^{4^+}}{E_g^{2^+}}$		2.48			2.29		
χ			11.33	17.84		9.88	15.41
A_1	a	522.4864	562.6938		649.8648	710.6779	
A_2	b	8.1960	0.273 8559		9.2391	0.329 923	
d	c	1.5466	$9.519\,95 \times 10^{-4}$		1.4174	$5.317\,905 \times 10^{-4}$	

5. Conclusions

In this section we summarize the main results obtained in this paper. By a dequantization procedure we associated with a quantum mechanical Hamiltonian that is quadratic in the quadrupole bosons, a time-dependent classical equation. The classical Hamiltonian has a separated form, i.e. a sum of a kinetic and a potential energy term. The latter is not dependent on momenta and is of Davidson type. We may say that our procedure proves the classical origin of the Davidson potential. The centrifugal term is determined by a pseudo-angular momentum associated with the intrinsic coordinates. It is worth mentioning that the constraint for the angular momentum in the laboratory frame yields a differential equation which is connected to that one corresponding to the energy conservation which results in obtaining a specific angular momentum dependence for the quantal energy. Actually the expression obtained generalizes the Holmberg–Lipas formula, involving a $J^2(J+1)^2$ term within the square root.

A similar expression was obtained by one author (AAR) within the CSM for a large deformation regime. Another compact expression was proposed by the CSM for the near-vibrational regime, i.e. small nuclear deformation. One of the targets of this paper was to prove that the two compact expressions provided by the CSM are able to describe the ground-state energies for deformed, near-vibrational and transitional nuclei. By matching the two expressions one obtains a unitary description for nuclei satisfying different symmetries or, in other words, belonging to various nuclear phases. A similar goal is achieved by using a square root formula, a generalization of the Holmberg–Lipas formula, obtained on the base of a semiclassical description.

These descriptions are used for a large number of nuclei (44). The agreement between results and experimental excitation energies is very impressive. The agreement quality is judged by the small rms values of discrepancies.

The nuclei chosen in our analysis cover nuclei ranging from near-vibrational to well-deformed nuclei and belonging to various symmetries. Thus, the nuclei in tables 2 and 3 are axially symmetric deformed nuclei except for ^{228}Th, which exhibits the features of a triaxial nucleus. The nuclei considered in tables 4 and 5 and the first two in table 6 represent the deformed branches of the nuclear phase transition $SU(5) \to SU(3)$, while the last three nuclei in table 6 belong to the side of the $O(6) \to SU(3)$ phase transition. Nuclei characterized by relatively small values of d are considered in tables 7–9. These satisfy different symmetries like $O(6)$ (table 7), $SU(5)$ (table 8) and $X(5)$ (table 9). The nuclei in table 10 seem to play the role of a critical point for the phase transition $SU(5) \to SU(3)$ in the respective isotopic chain. The two nuclei satisfying the symmetry $E(5)$ associated with the critical point of the phase transition $O(6) \to SU(5)$ are presented in table 11.

As a final conclusion we may say that the CSM procedure is able to describe in a realistic fashion the ground-state energies for nuclei of different nuclear phases. An alternative description is given by a square root formula derived as an approximate eigenvalue of a quadratic Hamiltonian in quadrupole bosons subject to a constraint due to the angular momentum conservation.

Acknowledgments

This work was supported by the Romanian Ministry for Education, Research, Youth and Sport through the CNCSIS projects ID-33/2007 and ID-946/2007.

Appendix A

Using the equations of motion for the conjugate variables, one can prove that

$$\dot{\mathcal{L}}_3 = 0, \qquad \dot{\mathcal{H}}_1 = 0, \tag{A.1}$$

where $\mathcal{L}_3$ is defined by the following expression:

$$\mathcal{L}_3 \equiv \frac{\hbar}{2}(q_1 p_2 - q_2 p_1) = \frac{\hbar^2}{A'} r^2 \dot{\theta}, \tag{A.2}$$

and has the significance of the third component of the angular momentum defined in the phase space, spanned by the coordinates (q_1, p_1, q_2, p_2). The other two components are

$$\mathcal{L}_1 = \frac{\hbar}{4}\left((q_1^2 + p_1^2 - q_2^2 - p_2^2\right), \qquad \mathcal{L}_2 = \frac{\hbar}{2}(q_1 q_2 + p_1 p_2). \tag{A.3}$$

Indeed, one can easily check that

$$\{\mathcal{L}_i, \mathcal{L}_k\} = \hbar \epsilon_{ikj} \mathcal{L}_l, \tag{A.4}$$

where $\{,\}$ denotes the Poisson bracket and ϵ_{ikj} the antisymmetric unit tensor. By virtue of equation (A.4) the set of functions $\mathcal{L}_k$ with the Poisson brackets as multiplication operation forms a classical $SU_c(2)$ algebra. Moreover, they could be obtained by averaging with $|\Psi\rangle$, the generators $\hat{L}_k$:

$$\mathcal{L}_k = \langle \Psi | \hat{L}_k | \Psi \rangle; \qquad k = 1, 2, 3, \tag{A.5}$$

of a boson $SU_b(2)$ algebra defined with the boson operators $b_0^\dagger$, $b_{\pm 2}^\dagger$, as

$$\begin{aligned}
\hat{L}_1 &= \frac{\hbar}{4}\left[2b_0^\dagger b_0 - \left(b_2^\dagger + b_{-2}^\dagger\right)(b_2 + b_{-2})\right], \\
\hat{L}_2 &= \frac{\hbar}{2\sqrt{2}}\left[b_0^\dagger (b_2 + b_{-2}) + \left(b_2^\dagger + b_{-2}^\dagger\right) b_0\right], \\
\hat{L}_3 &= \frac{\hbar}{2\sqrt{2}\mathrm{i}}\left[b_0^\dagger (b_2 + b_{-2}) - \left(b_2^\dagger + b_{-2}^\dagger\right) b_0\right].
\end{aligned} \tag{A.6}$$

Equation (2.15) and the correspondence between commutators and Poisson brackets, $[,] \to \frac{1}{i}\{,\}$, define a homeomorphism of the boson and classical algebras generated by $\{\hat{L}_k\}_{k=1,2,3}$ and $\{\mathcal{L}_k\}_{k=1,2,3}$, respectively. Note that the boson $SU_b(2)$ algebra does not describe the rotations in the real configuration space but in a fictitious space. The conservation law expressed by (A.1) is determined by the invariance against rotation around the third axis in the fictitious space mentioned above: $[H, \hat{L}_3] = 0$. Since the classical system is characterized by two degrees of freedom and, on the other hand, there are two constants of motion

$$\mathcal{H} = E, \qquad \mathcal{L}_3 = L, \tag{A.7}$$

the equations of motion are exactly solvable.

Appendix B

By direct calculations we can check that the overlap integral $I_J^{(0)}$ and its first and second derivatives satisfy the following differential equation:

$$\frac{\mathrm{d}^2 I_J^{(0)}}{\mathrm{d}x^2} - \frac{x-3}{2x}\frac{\mathrm{d}I_J^{(0)}}{\mathrm{d}x} - \frac{2x^2 + J(J+1)}{4x^2} I_J^{(0)} = 0 \quad (x = d^2). \tag{B.1}$$

By a suitable change of function this equation can be brought to the differential equation characterizing the hypergeometric function of the first rank. Thus, the final result for $I_J^{(0)}$ is

$$I_J^{(0)} = \frac{(J!)^2}{\left(\frac{J}{2}\right)!(2J+1)!}(6d^2)^{\frac{J}{2}}\,\mathrm{e}^{-\frac{d^2}{2}}\,{}_1F_1\left(\frac{1}{2}(J+1), J+\frac{3}{2}; \frac{3}{2}d^2\right). \tag{B.2}$$

This expression is further used for describing both the asymptotic and vibrational behavior for the excitation energies in the ground band. Indeed, in the asymptotic region of d, the hypergeometric function behaves like

$${}_1F_1(a, c; z) = \frac{\Gamma(c)}{\Gamma(a)}\mathrm{e}^z z^{a-c}[1 + \mathcal{O}(|z|^{-1})]. \tag{B.3}$$

Due to this expression the dominant term of $I_J^{(0)}$ is

$$I_J^{(0)} \sim \frac{\mathrm{e}^x}{3x}. \tag{B.4}$$

This expression suggests, for $I_J^{(0)}$, in the asymptotic region, the following form:

$$I_J^{(0)} = \mathrm{e}^x \sum_{n=1} A_n x^{-n}. \tag{B.5}$$

Inserting this expression into the above differential equation one obtains the recursion relation for the expansion coefficients A_k:

$$A_{n+1} = \frac{A_n}{6n}(2n + J)(2n - J - 1). \tag{B.6}$$

The leading term (B.4) gives $A_1 = \frac{1}{3}$ and then (B.6) determines the whole set of expansion coefficients. In this way we obtain for the ratio $d^2 I_J^{(1)}/I_J^{(0)}$ the expression

$$x\frac{I_J^{(1)}}{I_J^{(0)}} = x - 1 - \frac{1}{3x} - \frac{5}{9x^2} - \frac{37}{27x^3} + \left(\frac{1}{6x} + \frac{5}{18x^2} + \frac{13}{18x^3}\right) J(J+1)$$
$$- \frac{1}{54x^3} j^2(J+1)^2 + \mathcal{O}(x^{-4}). \tag{B.7}$$

The convergence in terms of x for the excitation energy may be improved in two steps. First we write the differential equation for $I_J^{(0)}$ in a different form:

$$x\left(x\frac{I_J^{(1)}}{I_J^{(0)}}\right)' + \left(x\frac{I_J^{(1)}}{I_J^{(0)}}\right)^2 - \frac{x-1}{2}\left(x\frac{I_J^{(1)}}{I_J^{(0)}}\right) - \frac{2x^2+J(J+1)}{4} = 0. \tag{B.8}$$

The derivative $\left(x\frac{I_J^{(1)}}{I_J^{(0)}}\right)'$ is further calculated by using (B.7) and thus the above equation becomes a second-degree algebraic equation for $x\frac{I_J^{(1)}}{I_J^{(0)}}$. Solving this equation one obtains

$$x\frac{I_J^{(1)}}{I_J^{(0)}} = \frac{1}{2}\left[\frac{x-2}{2} + \sqrt{G_J}\right], \tag{B.9}$$

where we used the notation

$$G_J = \frac{9}{4}x(x-2) + \left(J+\frac{1}{2}\right)^2 - \frac{4}{9x}\left(3+\frac{10}{x}+\frac{37}{x^2}\right) + \frac{2}{3x}\left(1+\frac{10}{3x}+\frac{13}{x^2}\right)J(J+1) - \frac{2J^2}{9x^3}(J+1)^2. \tag{B.10}$$

Concerning the near-vibrational regime the final expression for energies is obtained in two steps. First one derives the vibrational limit of the kth derivative:

$$\lim_{d\to 0}\left(d^2\frac{I_J^{(1)}}{I_J^{(0)}}\right)^{(k)} = \frac{1}{(2J+3)^k}\left[\frac{J}{2}(\delta_{k,0}+\delta_{k,1}) + 9\frac{(J+1)(J+2)}{2J+5}\left((\delta_{k,2}+9\frac{\delta_{k,3}}{2J+7}\right)\right], \qquad k=0,1,2,3. \tag{B.11}$$

Then, truncating the Taylor expansion of $x\frac{I_J^{(1)}}{I_J^{(0)}}$, around the point $x=0$, at the third order one obtains

$$x\frac{I_J^{(1)}}{I_J^{(0)}} = \frac{J}{2} + \frac{J}{2(2J+3)}x + \frac{9}{2}\frac{(J+1)(J+2)}{2J+3)^2(2J+5)}x^2 + \frac{27}{2}\frac{(J+1)(J+2)}{(2J+3)^3(2J+5)(2J+7)}x^3 + \mathcal{O}(x^4). \tag{B.12}$$

References

[1] Mariscotti A A J, Scharff-Goldhaber G and Buch B 1969 *Phys. Rev.* **178** 1864
[2] Harris S M 1965 *Phys. Rev.* B **138** 509
[3] Das T D K, Dreizler R M and Klein A 1970 *Phys. Rev.* C **2** 632
[4] Holmberg P and Lipas P O 1968 *Nucl. Phys.* A **117** 552
[5] Davidson P M 1932 *Proc. R. Soc.* A **135** 459
[6] Raduta A A and Sabac C 1983 *Ann. Phys., NY* **148** 1–31
[7] Raduta A A, Stoica S and Sandulescu N 1984 *Rev. Roum. Phys.* **29** 55
[8] Arima A and Iachello F 1976 *Ann. Phys., NY* **91** 253
[9] Arima A and Iachello F 1976 *Ann. Phys., NY* **123** 468
[10] Casten R F 1981 *Interatcting Bose–Fermi Systems in Nuclei* ed F Iachello (New York: Plenum) p 1
[11] Iachello F 2000 *Phys. Rev. Lett.* **85** 3580
[12] Iachello F 2001 *Phys. Rev. Lett.* **87** 052502
[13] Raduta A A, Ceausescu V, Gheorghe A and Dreizler R M 1982 *Nucl. Phys.* A **381** 253
[14] Raduta A A and Faessler A 2005 *J. Phys. G: Nucl. Part. Phys.* **31** 873–901
[15] Raduta A A, Gheorghe A and Faessler A 2005 *J. Phys. G: Nucl. Part. Phys.* **31** 337–53

[16] Gheorghe A C, Raduta A A and Faessler A 2007 *Phys. Lett.* B **648** 171–5
[17] Raduta A A, Gheorghe A C, Buganu P and Faessler A 2009 *Nucl. Phys.* A **819** 46–78
[18] Artna-Cohen A 1997 *Nucl. Data Sheets* **80** 723
[19] Schmorak M R 1991 *Nucl. Data Sheets* **63** 139
[20] Akovali Y A 1994 *Nucl. Data Sheets* **71** 181
[21] Schmorak M R 1991 *Nucl. Data Sheets* **63** 183
[22] Chukreev F E, Makarenko V E and Martin M J 2002 *Nucl. Data Sheets* **97** 129
[23] Chukreev F E and Singh B 2004 *Nucl. Data Sheets* **103** 325
[24] Akovali Y A 2002 *Nucl. Data Sheets* **96** 177
[25] Akovali Y A 1999 *Nucl. Data Sheets* **87** 249
[26] Reich C W and Helmer R G 1998 *Nucl. Data Sheets* **85** 171
[27] Reich C W 2003 *Nucl. Data Sheets* **99** 753
[28] Helmer R G 2004 *Nucl. Data Sheets* **101** 325
[29] Reich C W 1996 *Nucl. Data Sheets* **78** 547
[30] Helmer R G and Reich C W 1999 *Nucl. Data Sheets* **87** 317
[31] Singh B 2001 *Nucl. Data Sheets* **93** 243
[32] Shurshikov E N and Timofeeva N V 1992 *Nucl. Data Sheets* **67** 45
[33] Singh B 1995 *Nucl. Data Sheets* **75** 199
[34] Browne E and Junde H 1999 *Nucl. Data Sheets* **87** 15
[35] Browne E and Junde H 1998 *Nucl. Data Sheets* **84** 337
[36] Singh B and Firestone R B 1995 *Nucl. Data Sheets* **74** 383
[37] Baglin C M 2003 *Nucl. Data Sheets* **99** 1
[38] Browne E 1994 *Nucl. Data Sheets* **72** 221
[39] Wu S-C and Niu H 2003 *Nucl. Data Sheets* **100** 483
[40] Baglin C M 2002 *Nucl. Data Sheets* **96** 611
[41] Blachot J 2000 *Nucl. Data Sheets* **91** 135
[42] derMateosian E and Tuli J K 1995 *Nucl. Data Sheets* **75** 827
[43] Artna-Cohen A 1996 *Nucl. Data Sheets* **79** 1
[44] Blachot J 1991 *Nucl. Data Sheets* **64** 1
[45] De Frenne D and Jacobs E 1998 *Nucl. Data Sheets* **83** 535